Astron. Astrophys. 357, 1013–1019 (2000)

ASTRONOMY AND ASTROPHYSICS

The C–C–C bending modes of PAHs: a new emission plateau from 15 to 20 μm

C. Van Kerckhoven[1], S. Hony[2], E. Peeters[3,4], A.G.G.M. Tielens[4,3], L.J. Allamandola[5], D.M. Hudgins[5], P. Cox[6], P.R. Roelfsema[3], R.H.M. Voors[7], C. Waelkens[1], L.B.F.M. Waters[2,1], and P.R. Wesselius[3]

[1] Instituut voor Sterrenkunde, K.U. Leuven, Celestijnenlaan 200B, 3001 Heverlee, Belgium
[2] Astronomical Institute "Anton Pannekoek", Kruislaan 403, 1098 SJ Amsterdam, The Netherlands
[3] SRON, P.O. Box 800, 9700 AV Groningen, The Netherlands
[4] Kapteyn Astronomical Institute, P.O. Box 800, 9700 AV Groningen, The Netherlands
[5] NASA-Ames Research Center, Space Science Division, MS: 245-6, Moffett Field, CA 94035-1000, USA
[6] Institut d'Astrophysique Spatiale, Université Paris XI, 91405 Orsay, France
[7] Sterrenkundig Instituut, Universiteit Utrecht, Princetonplein 5, 3584 CA Utrecht, The Netherlands

Received 5 November 1999 / Accepted 17 March 2000

Abstract. We have obtained 2.5–45 μm spectra of a sample of compact H II regions, YSOs and evolved stars in order to study the origin and evolution of interstellar Polycyclic Aromatic Hydrocarbon molecules (PAHs). Besides the well–known, strong PAH bands at 3.3, 6.2, 7.7, 8.6, and 11.2 μm, these spectra reveal for the first time, a ubiquitous emission plateau from 15 to 20 μm. While the overall shape of this plateau is very similar in all sources, the detailed profiles vary from source to source. In particular, some sources show a distinct emission feature at 16.4 μm. Moreover, the integrated intensity of this plateau varies relative to the PAH emission features by a factor 10 in our sample.

We attribute this 15–20 μm plateau to a blend of many emission features due to the interstellar or circumstellar PAH family present in these sources. Laboratory studies and quantum chemical calculations show that PAH molecules invariably possess emission features in this wavelength region, arising from C–C–C bending modes which cause in– and out–of–plane distortion of the carbon skeleton. These modes are very sensitive to the molecular structure of the specific PAHs present and hence different molecules emit at different wavelengths. Analysis of the available data on the IR characteristics of PAHs show that a collection of PAHs will give rise to a broad plateau in this region.

We have analyzed the size distribution of PAHs giving rise to the IR emission spectra of the sources in our samples. While much of the 15–20 μm plateau is thought to arise in relatively large PAHs and PAH clusters, we attribute the 16.4 μm feature to the small end of the interstellar PAH size distribution. We conclude that the observed increased strength of the 15–20 μm plateau relative to the shorter wavelength IR emission features in regions of massive star formation is caused by a preponderance of larger PAHs and PAH clusters in those sources. Possibly this reflects the importance of coagulation in the dense molecular cloud environment from which these stars are formed.

Send offprint requests to: C. Van Kerckhoven (caroline@ster.kuleuven.ac.be)

Key words: ISM: molecules – ISM: dust, extinction – ISM: H II regions – ISM: planetary nebulae: general – stars: pre-main sequence – infrared: ISM: lines and bands

1. Introduction

Ground–based, airborne, and space–based observations have shown that the mid–infrared spectra of many objects with associated dust and gas are dominated by the well-known emission features at 3.3, 6.2, 7.7, 8.6, and 11.2 μm (Gillett et al. 1973; Cohen et al. 1986; Geballe et al. 1985; Roche et al. 1989; Roelfsema et al. 1996; Beintema et al. 1996). These bands are now generally attributed to vibrational relaxation of UV–pumped Polycyclic Aromatic Hydrocarbon molecules (PAHs) containing $\simeq$50 carbon atoms (Allamandola et al. 1989, hereafter ATB; Léger & Puget 1984, 1989; Tielens et al. 1999). The PAH molecules do not only dominate the IR spectral characteristics of the ISM, they also play an important role in the life cycle of the interstellar medium. The photoelectric effect on PAHs and PAH clusters dominates the heating of diffuse interstellar gas and therefore, PAHs are an essential ingredient of the phase structure of the ISM. Because of their large abundance, PAHs are also important for the charge balance inside dense interstellar clouds and hence they regulate important processes such as ambipolar diffusion (Lepp & Dalgarno 1988). Finally, interstellar PAHs and PAH clusters provide a large surface area for reactions, leading to the formation of H_2 and other species (Allen & Robinson 1975). The origin and evolution of the interstellar medium is therefore intimately interwoven with the origin and evolution of interstellar PAHs.

The ISO mission[1] was ideally suited to study these IR emission features spectroscopically in a large variety of objects. We

[1] The ISO mission was an ESA project with instruments funded by ESA member states (especially the PI countries: France, Germany, the Netherlands, and the United Kingdom) and with participation of ISAS and NASA.

Table 1. Log of ISO observations

Object	observer	AOT	Date	Rev.	$\alpha(2000)$	$\delta(2000)$	JD-2 450 000
IRAS 18502+0051	pcox	SWS 01(2)	17-04-1996	152	18h52m50.21s	– 00h55m27.59s	191.05
IRAS 23030+5958	pcox	SWS 01(2)	23-06-1996	220	23h05m10.57s	+60h14m40.60s	258.52
IRAS 15384-5348	pcox	SWS 01(2)	10-09-1996	299	15h42m17.16s	– 54h01m28.49s	337.24
IRAS 23133+6050	pcox	SWS 01(2)	23-06-1996	220	23h15m31.44s	+61h07m08.51s	258.73
IRAS 22308+5812	pcox	SWS 01(2)	12-05-1996	177	22h32m45.95s	+58h28m21.00s	216.13
IRAS 18317-0757	pcox	SWS 01(2)	08-03-1997	478	18h34m24.94s	– 08h05m12.08s	516.21
S106 IRS4	pwesseli	SWS 01(2)	16-10-1996	335	20h27m26.68s	+37h22m47.89s	373.73
IRAS 03260+3111	cwaelken	SWS 01(3)	04-09-1997	659	03h29m10.37s	+31h21m58.28s	696.86
CD-42 11721	rvoors	SWS 01(2)	23-08-1997	647	16h59m06.80s	– 43h17m52.01s	684.97
NGC7027	sws_cal	SWS 01(4)	11-12-1995	24	21h07m01.71s	+42h14m09.10s	63.21

have initiated a project to study the origin and evolution of PAH molecules in compact H II regions, young stellar objects – in particular Herbig AeBe stars – and stars in the later stages of their evolution (post–AGB objects and planetary nebulae (PNe)) using 2.5–45 μm spectra obtained with the Short Wavelength Spectrometer (SWS) on board of ISO. In all there are about 75 sources in the combined samples. First results of these studies have been presented in Roelfsema et al. (1996), Molster et al. (1996), Tielens et al. (1999), Cox et al. (1999), Van Kerckhoven et al. (1999), and Peeters et al. (1999).

PAH molecules will show emission longward 15 μm associated with the bending modes of the carbon–skeleton (ATB; Zhang et al. 1996; Moutou et al. 1996). For small molecules, these modes are more molecule specific than the modes giving rise to the shorter wavelength features and hence the 15–20 μm region holds great promise from a molecular identification point of view. Here we discuss the infrared characteristics in the 15–20 μm region of a subset of the sources in the samples. In Sect. 2, we present the Short Wavelength Spectrometer (SWS) observations of the sources in our sample. The characteristics of the newly discovered 15–20 μm plateau are discussed in Sect. 3. The infrared spectroscopy of PAH molecules in this wavelength region are reviewed in Sect. 4. Finally, in Sect. 5, the implications of this plateau for the interstellar PAH size distribution are considered. Our results are summarized in Sect. 6.

2. Observations and reduction

We present observations taken with the Short Wavelength Spectrometer (SWS) on board the Infrared Space Observatory (ISO) (see Table 1). All spectra were taken using the AOT1 scanning mode at various speeds, with resolving power ($\Delta\lambda/\lambda$) ranging from 500–1500. The data were processed using SWS Interactive Analysis (de Graauw et al. 1996); IA^3 using calibration files and procedures equivalent with pipeline version 7.0. Further data processing consisted of bad data removal, rebinning with a constant resolution and splicing the subbands to form a continuous spectrum. The amount of shifting between subbands is within the calibration uncertainties for the region of interest. The shifting mostly influences the strength of the emission plateaus, but has little influence on the shape.

In some cases, even after bad data removal, the spectra still suffer from noise due to glitches. The features discussed here are present in all available scans.

We only consider spectra with an emission plateau which satisfies the following conditions:

1. The emission plateau has to be detectable in both up and down scan.
2. The change in slope has to occur within one subband, not at the bandedges.
3. The slope in overlapping parts of the different subbands has to be the same.
4. The shifting of the subbands required to form a continous spectrum has to be within the calibration uncertainties.

3. The 15–20 μm plateaus

Many of the observed sources in our samples show a broad plateau between 15 and 20 μm. Fig. 1 shows two examples in which the plateau is clearly present.

3.1. Continuum

To be able to compare the plateaus observed in different sources we locally subtract a spline continuum. The rising dust continuum and the presence of features at both shorter and longer wavelength give some freedom in drawing a continuum. This mostly affects the strength of the plateau, but has only a minor influence on the shape. We estimate that this introduces an uncertainty of, at most, 30% in the plateau strength. An exception to this is the young planetary nebula NGC 7027 where the presence of a strong 30 μm feature at the long wavelength side of the plateau makes the extent and the strength of the plateau more difficult to determine.

3.2. The shape of the plateaus

The continuum subtracted profiles are shown in Fig. 2. Overall, the profile of the plateau is very similar between the different sources (see Fig. 3). However, when examined in detail, some small, but significant differences become apparent. Three sources show a distinct feature at 16.4 μm (NGC 7027, CD 42, IRAS 03260; Fig. 4), which may be present in others as well

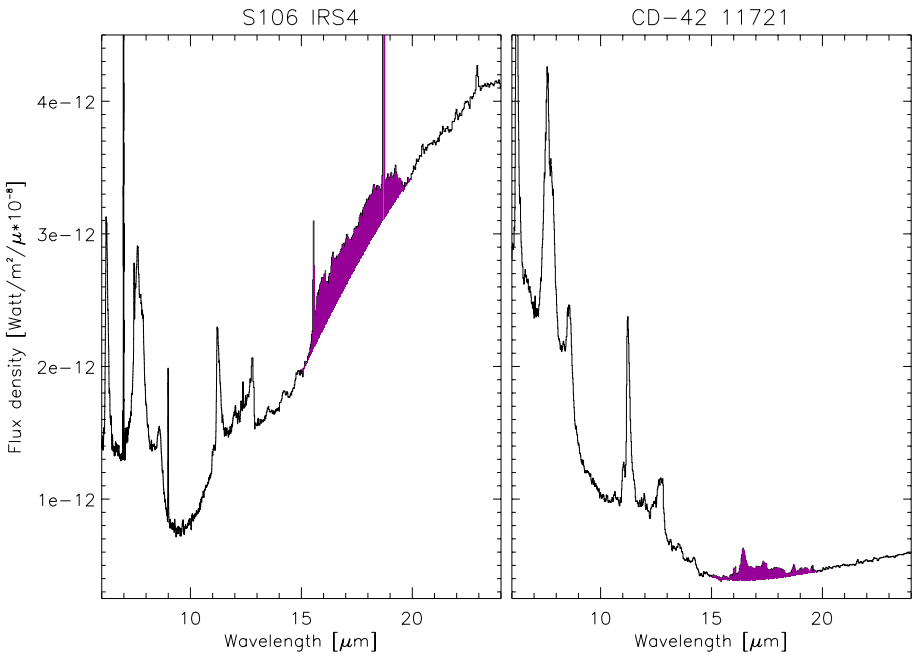

Fig. 1. Two clear examples of the 15–20 μm plateau. The 15–20 μm emission plateau is highlighted through shading.

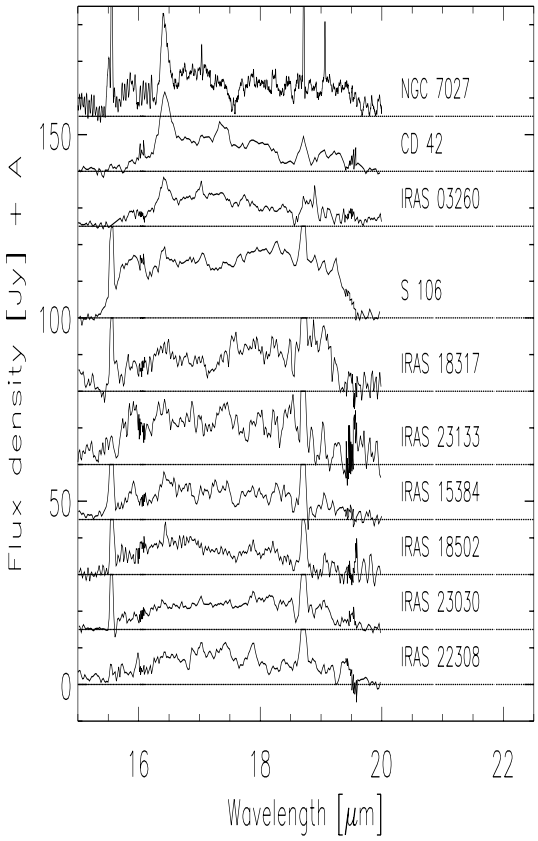

Fig. 2. Continuum subtracted spectra in the 15 to 20 μm region. S 106 and NGC 7027 are scaled by a factor 0.5. For clarity the strong [Ne III] and [S III] lines at 15.55 and 18.7 μm are truncated. The sources in the three upper panels have a strong 16.4 μm band.

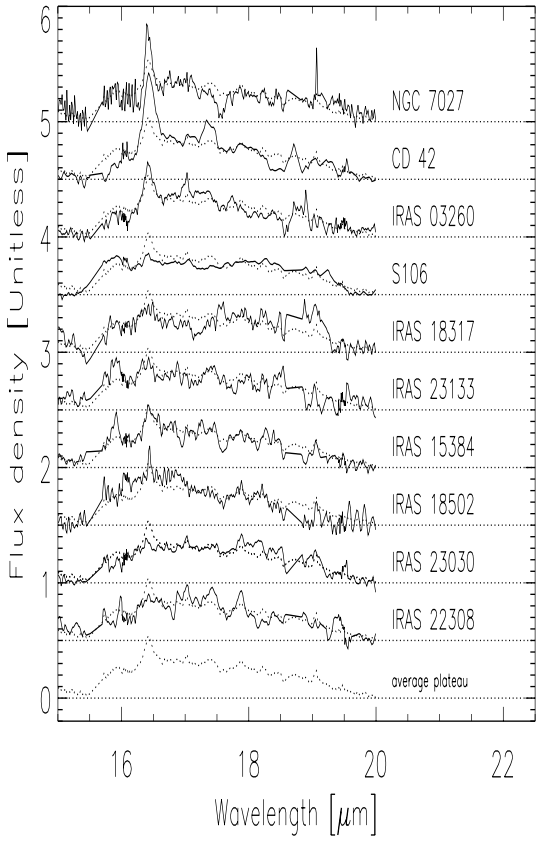

Fig. 3. Continuum subtracted spectra in the 15 to 20 μm region. The intensity of plateau is scaled to unity. All spectra are overplotted with the average of all normalized plateaus. The strong [Ne III] and [S III] lines at 15.55 and 18.7 μm have been removed.

(IRAS 15384, S 106, IRAS 23133, IRAS 18502), but is not apparent in all. This feature has also been observed by Moutou et al. (1999) in the reflection nebula NGC 7023. The latter paper also reports a feature at 15.8 μm. While this feature does not

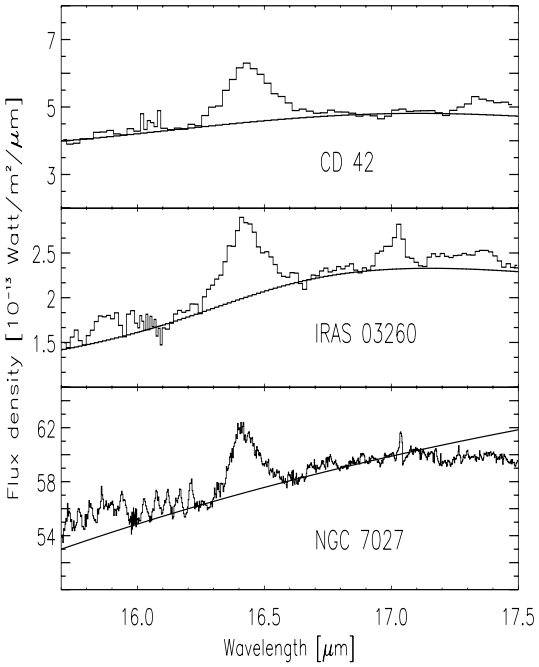

Fig. 4. The spectra of three sources with a clear 16.4 μm feature. The full drawn lines show the continua we adopted to measure the 16.4 μm feature.

stick out immediately in our sample, comparison of the profiles in IRAS 03260, IRAS 23133 and S 106 suggests the presence of a 15.8 μm feature in the latter two. The presence of a dip in the plateau of NGC 7027 at 17.5 μm suggests the presence of distinct components around 17 μm and perhaps 18 μm. We note that around this wavelength, CD 42 and IRAS 23133 show a weak emission feature. The profile of the plateau may also differ around 19 μm but that depends to some extent on the adopted continuum, which is not always well established.

Sources which show the PAH bands in their spectra, often show a plateau of emission extending from 15 to about 20 μm. The plateau may well be present in all the sources of our PAH samples but difficult to recognize because of strong, rising dust continua in some and the presence of spectral structure due to crystalline silicates in others. However, the 15–20 μm emission plateau is not detected in sources characterized by only O–rich dust such as O–rich AGB stars (Molster et al. 1999; Sylvester et al. 1999; Voors 1999) and we conclude that the carrier of this plateau is carbonaceous in origin. Finally, from the observed spectral variations in our sample, we interpret this plateau as a collection of blended emission features.

3.3. Integrated strength of the plateaus

The H II regions of the sample have strong [Ne III] and [S III] lines at 15.55 and 18.7 μm. These lines are removed prior to the integrated strength measurements. The intensities listed in Table 2 are obtained by integrating the continuum subtracted fluxes between 15.2 and 20 μm . Perusal of this table shows that the integrated strength of the plateau is highly variable relative to the C–C stretching mode at 6.2 μm ($I_{plateau}/I_{6.2}$ = 0.6–4.4) and the C–H out of plane bending mode at 11.2 μm ($I_{plateau}/I_{11.2}$ = 0.5–5.5; see Fig. 1).

Table 2. Integrated strength of the features

Source	$I^{a,b}_{plateau}$	$I^{a,c}_{6.2}$	$I^{a,c}_{11.2}$	$I^{a,c}_{16.4}$	Object[d]
IRAS 18502+0051	22.6	9.69	12.4	y	CH II
IRAS 23030+5958	22.8	6.46	7.81	n	CH II
IRAS 15384-5348	25.6	27.6	13.4	y	CH II
IRAS 23133+6050	43.2	25.5	18.3	y	CH II
IRAS 22308+5812	24.3	11.9	9.76	n	CH II
IRAS 18317-0757	35.5	27.1	13.3	n	CH II
S106-IRS4	119.	27.2	21.5	y	H II
IRAS 03260+3111	22.8	24.0	20.1	1.34	HAeBe
CD-42 11721	25.8	40.9	33.3	3.65	HAeBe
NGC 7027	72.7	91.2	141.	6.16	PN

[a] Intensities are listed in $10^{-14}W/m^2$.
[b] Uncertainty less than 30%.
[c] Uncertainty less than 20%.
[d] (C)H II = (compact) H II region, HAeBe = Herbig Ae/Be star, PN = planetery nebula

4. C–C–C bending modes of PAHs

Within the framework of the PAH model, emission is expected longward of about 15 μm arising from the C–C–C bending modes which cause in- and out-of-plane distortion of the carbon skeleton. Given that these PAH modes are spread out over this region, but tend to congest at the shorter wavelength end, a low-lying, long wavelength continuum emission was expected from PAH sources since all PAHs—large and small—will emit here (ATB). This initial expectation was based on a very limited set of laboratory PAH spectra, comprised principally of small species (C_{10} to C_{24}). In recent years, many more PAHs have been measured in the laboratory and they consistently show IR modes in this wavelength region. Hudgins and coworkers (e.g. Hudgins & Sandford 1998, and references therein) have reported the spectra of 23 neutral and 20 cationic PAHs between 2.5 and 20 μm isolated in rare gas matrices at 10 K. Moutou et al.(1996) present a Far IR spectral collection of about 40 neutral PAHs suspended in CsI pellets between 14 and 40 μm. Further, Zhang et al. (1996) have directly studied the far-IR emission of a few PAHs in the gas phase. Together, these data allow us to refine the earlier expectations. Overall, the individual bands in this region typically have intensities no more than 5–10% of the most intense bands in the spectrum (ATB; Langhoff 1996; Hudgins & Sandford 1998 and references therein). Consider, for example, the fluoranthenes, a PAH family defined by the incorporation of a pentagonal cyclopentadienyl ring in their carbon skeletons. For the neutral fluoranthenes individual band intensities in the 15 to 30 μm region typically range from a few to 10% those of the dominant C–H out-of-plane bends in the 11 to 15 μm range and are comparable to the C–C stretches in the 6 μm region. The laboratory data also shows that, despite the dramatic effect of ionization on the global band intensity pattern across the mid–

IR, the absolute intensities of the bands in the 15–30 μm range are only moderately affected, if at all, by ionization. Specifically, absorption intensities lie in the range 2–30 km/mol for neutral PAHs and 6–30 km/mol for PAH cations (Langhoff 1996). Bearing in mind that a PAH has typically between 3 and 10 features in this wavelength region, the total integrated strength from all of these long wavelength features taken together exceeds that of the 6.2 μm band.

Fig. 5 shows the average of the observed plateaus reported here, compared to the broad feature produced by simply coadding the laboratory absorption spectra of a few molecules from the Hudgins dataset, assigning each band a roughly 30 wavenumber width as expected for emission from highly vibrationally excited molecules (ATB). The specific molecules chosen to produce the broad laboratory feature is not unique. Given that larger interstellar molecules up to sizes of 10^4 C–atoms can contribute to this region as well (Schutte et al. 1993), a pseudo continuum (emission plateau) is indeed expected as part of the PAH model.

While there is some variation in the substructure of the emission plateaus observed, there is a distinct, slightly stronger component centered near 16.4 μm in some sources (Fig. 4). Infrared activity in this spectral region corresponds to in-plane C-C-C bends whereas bands longward of about 17 μm correspond to out-of-plane warping (Bauschlicher, private communication). Of the molecules represented in the Moutou et al. and Hudgins et al. datasets, the species which consistently show a band between 16 and 17 μm which could build up and generate a striking feature at this location are the fluoranthenes (cf. mix 2, Fig. 5). Analysis of the specific vibrations corresponding to each feature in this region for these molecules (Bauschlicher, private communication) indicates that the prominent 16.4 μm band may arise from the vibration of a pendant hexagonal ring (not pentagonal ring, although these may have a band here in some cases) and in the cases studied here, most of the intensity at this position involves an in-phase, planar vibration of the two opposite carbons of the pendant ring (i.e. at the para positions) along the line which is parallel and adjacent to the fused bond with the rest of the molecule's carbon network (see Fig. 6). Analysis of the vibrations of molecules, without a pentagonal ring, but showing a band near 16.4 μm confirms the vibration of a pendant ring as origin of this band. We note that all of the fluoranthenes in the NASA Ames dataset possess a very strong band near 14 μm because they contain hexagonal rings, included the pendant ring responsible for the band near 16.4 μm, with 4–adjacent hydrogen atoms. Since these are small molecules, this dominates the spectrum in the CH out–of–plane region between 10.5 and 14 μm. There is a weak feature at this position in the interstellar spectra (Hony et al. in preparation). Nevertheless, the smallest members of the fluoranthene family cannot be major carriers of the interstellar 16.4 μm emission band. Alternatively, the distinctive symmetry of the pentagonal ring might just induce IR activity in otherwise weak or forbidden transitions and, as such, pentagons may represent only one possible way in which broken symmetry can lead to enhanced IR activity at this position. If the latter is the case, this effect may also become particularly important for asymmetric, non-condensed PAHs. This distinctive substructure is likely a characteristic of smaller PAHs because, as PAH species increase in size, the influence of the center of asymmetry in a molecule on its spectrum becomes diluted by the constant increase in the number of regular PAH modes.

In summary, together with the laboratory data discussed in this section, the astronomical detection of the 15–20 μm feature reported in this paper provides further credence to the PAH model and can be used to deduce specific characteristics of the interstellar PAH population in various regions. Substructure in the plateau, such as the 16.4 μm feature, may be particularly useful in this respect since they are likely carried by the small end of the PAH size distribution.

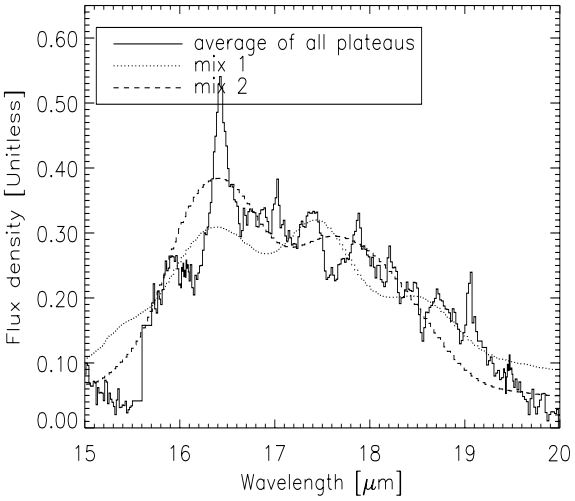

Fig. 5. Comparison between the average of all plateaus and laboratory spectra. The average was obtained by coadding all interstellar emission plateaus normalized to the integrated intensity. The first laboratory spectrum (mix 1) is produced by the coadded spectra of anthracene (33%), 1,2-benzo(a)anthracene (33%), and pentacene (33%). The second laboratory spectrum (mix 2) is a spectrum produced by the mixture: benzo(k)fluoranthene (20%), pentacene (40%), anthracene (20%), and 1,2 benzanthracene (20%). The clear feature around 16.4 μm in the second laboratory spectrum is caused by the two fluoranthenes.

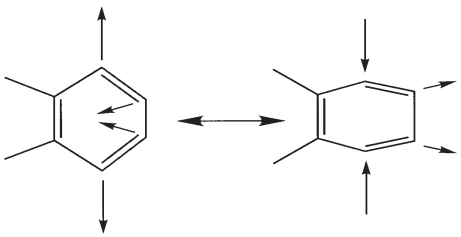

Fig. 6. The in-plane C–C–C bending of the pendant ring that characterizes vibrational modes near 16 μm. The intensity at this position involves an in-phase, planar vibration of the two opposite carbons of the pendant ring (i.e. at the para positions) along the line which is parallel and adjacent to the fused bond with the rest of the molecule's carbon network.

5. The size distribution of interstellar PAHs

The observed spectrum of IR emission features can be used to determine the sizes and abundances of the emitting species (ATB). Here, we are particularly interested in the observed variations from source to source in the strength of the 15–20 μm plateau relative to the PAH bands. These variations span a factor 10 (see Table 2) which is much larger than expected from laboratory or theoretical calculations on the intrinsic strength of modes in this wavelength region. Here we use a simple model to show that these variations can be attributed to changes in the size distribution.

Theoretical calculations have shown that PAHs with sizes up to $\simeq 10^4$ C–atoms can contribute to the emission in the 15–20 μm range (Schutte et al. 1993). Typically, we expect the emission in the 15–20 μm plateau to be dominated by those PAHs/PAH–clusters whose temperature upon absorption of a UV photon is best matched to this wavelength region (ie., $N_c \sim 2000$; ATB). For comparison, the bands at 3.3, 6.2, 7.7 and 11.2 μm are carried by PAHs in the size range 20 to a few hundred, while the 6–9 μm plateau underneath the 6.2 and 7.7 μm features is mainly due to PAHs with $N_c \sim 500$ C–atoms (ATB). Adopting standard dust parameters and measured UV absorption cross sections for the PAHs (ATB), the abundance of carbon, f_C, locked up in the carriers of given spectral features – ie., PAHs of different sizes – can be derived from the ratio of the flux in these features to the total dust continuum, f_{IR},

$$f_C \simeq 90 \, \frac{7 \times 10^{-18}}{\sigma_{uv}} \frac{f_{IR}}{1 - f_{IR}} \quad ppm, \tag{1}$$

where σ_{uv} is the UV absoption cross section per C-atom ($\sigma_{uv} = 7 \times 10^{18}$ cm^{-2} per C–atom (Joblin et al. 1992)) and the abundance is given in parts per million relative to H. We have calculated these fractional abundances for the carriers of the PAH bands, 6–9 μm plateau and 15–20 μm plateau for the sources presented in this paper using our own SWS data and the LWS data obtained for these sources through parallel ISO programs. The results are presented in Fig. 7 for the two extremes in our sample, NGC 7027 and S 106. The PAH emission in NGC 7027 originates from a region of $\simeq 10''$ (Graham et al. 1993), completely contained within the SWS beam. S 106 is somewhat extended compared to the SWS beam but analysis of ISOCAM images in the PAH features suggests that only a small fraction of the flux in the PAH bands is missing in the SWS spectrum (Joblin et al. in preparation). The Far–IR dust emission is well contained within the LWS beam.

The abundance of carbon locked up in small (20–100) PAHs is calculated to be an order of magnitude higher in NGC 7027 than in S 106 (Fig. 7). Not only do the absolute abundances differ, the relative abundance from big to small PAHs changes even more between the two objects. It seems that, where NGC 7027 has most of its carbon locked up in small PAHs, these little ones are less important in S 106. The increased importance of large species is readily apparent when comparing the observed spectrum of S 106 with that of other sources (see Fig. 2). Although there are variations from source to source, most of the H II regions have abundances and abundance patterns similar

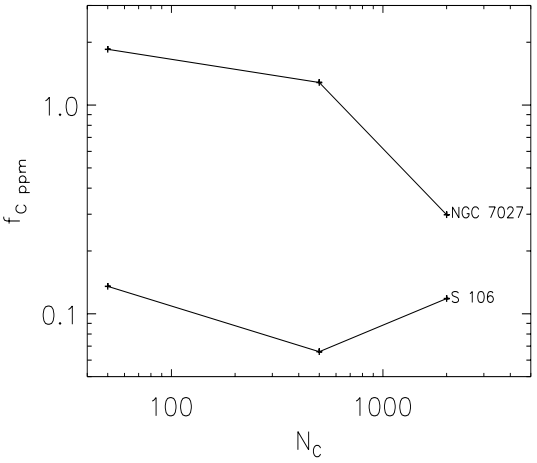

Fig. 7. Fraction of carbon locked up in PAH molecules of different sizes in units of parts per million relative to H. See text for details.

to S 106. In contrast, the YSOs, CD 42 and IRAS 03260, have considerably higher abundances of small PAHs relative to big PAH clusters, and resemble the PN, NGC 7027, in that respect. These variations in the size distribution of small species may reflect the extent to which coagulation has progressed during the formation of these different classes of sources. In particular, the Herbig AeBe stars, CD 42 and IRAS 03260, were probably formed from molecular cloud cores which were less dense than those that formed the much more massive stars at the center of H II regions. Coagulation may also have played less of a role in the ejecta of NGC 7027. We note that this interpretation of the observed variations in plateau to PAH band strength in terms of variations in the size distribution is supported by the assignment of the 16.4 μm band – so prominent in NGC 7027, CD 42 and IRAS 03260 – to small PAHs (cf., Sect. 4).

6. Summary

We have observed an emission plateau which extends from 15 to 20 μm in some young stellar objects, compact H II regions, and evolved objects (planetary nebulae) which show the PAH bands. The relative strength of this plateau, relative to the shorter wavelength PAH bands varies by about a factor 10 between the different sources. Although the global profile of the plateau is very similar between the different sources, significant variations in the substructure are apparent. The two YSO's, IRAS 03260 and CD 42, and the PN, NGC 7027, exhibit a clear 16.4 μm feature on top of this plateau, which contains about 10% of the total flux in the plateau. Taking this all together, we interpret this plateau as a collection of blended emission features carried by the same family of PAH molecules and PAH clusters responsible for the PAH bands and the 6–9 μm plateau underlying the 6.2 and 7.7 μm feature.

Using laboratory experimental spectra taken from the Hudgins dataset, and quantum chemical calculations preformed by Bauschlicher on the IR modes expected in this wavelength region for neutral and cationic PAHs, we show that bands in this wavelength region arise from C–C–C bending modes which

cause in– and out–of–plane distortions of the carbon skeleton. These C–C–C bending modes are very sensitive to the individual molecular structure of the PAH and, hence, different molecules emit at (slightly) different positions. A family of PAHs will therefore give rise to a plateau in this region (see Fig. 5.). Spectral substructure present in this plateau, such as the 16.4 μm band, seems to be a characteristic of the presence of asymmetry in the molecular structure, such as a pentagon, which tends to produce IR spectral activity around this wavelength. In that case, this band is likely carried by relatively small PAHs ($\simeq$ 50 C–atoms). Further laboratory and/or quantum chemical calculations may well provide important clues to the identity of the emitting species.

Following theoretical studies of the IR emission of a size distribution of PAHs, we attribute the overall 15–20 μm plateau emission to relatively large PAHs or PAH clusters containing typically $\simeq$ 2000 carbon–atoms (but recognizable spectral structure is likely carried by smaller species; see above). The intensity ratio of the 15–20 μm plateau to the UIR features is then a measure for the relative abundances of big PAH clusters and small PAH molecules. We can therefore attribute the observed variations in this ratio, to variations in the size distribution of PAHs and PAH clusters. Analysis of our data shows that the size distribution shifts to larger sizes in H II regions such as S 106 compared to the Herbig AeBe stars in our sample or to the PN, NGC 7027. Possibly, this reflects the effects of coagulation which may have been more important in the dense environment which lead to massive star formation than in regions where intermediate mass stars form. Whether the dominance of small sizes in the PNe, NGC 7027, reflects the irrelevance of coagulation in this environment or the effects of shattering in the (weak) shocks associated with its outflows is presently not clear.

Acknowledgements. CVK is a Research Assistant of the Fund for Scientific Research - Flanders. LBFMW and RHMV acknowledge financial support from a NWO 'Pioneer' grant. E.P. acknowledges the support from an NWO program subsidy (grant number 783-70-000). DMH and LJA gratefull, acknowledge support under NASA's IR Laboratory astrophysics (344-02-06-01) and Long Term Space astrophysics (399-20-01) programs.

References

Allamandola L.J., Tielens A.G.G.M., Barker J.R., 1989, ApJS 71, 733
Allen M., Robinson W.G., 1975, ApJ 195, 81
Beintema D.A., van den Ancker M.E., Molster F.J., et al. 1996, A&A 315, L369
Cohen M., Dopita M.A., Schwartz R., 1986, ApJ 302, 737
Cox P., Roelfsema P.R., Baluteau J.-P., et al., 1999, In: Cox P., Kessler M.F. (eds.) The universe as seen by ISO. ESA-SP 427, p. 631
de Graauw Th., Haser L.N., Beintema D.A., et al., 1996, A&A 315, L49
Geballe T.R., Lacy J.H., Persson S.E., et al., 1985, ApJ 292, 500
Gillett F.C., Roest W.J., Merril K.M., 1973, ApJ 183, 87
Graham J.R., Serabyn E., Herbst T.M., et al., 1993, AJ 105, 250
Hudgins D.M., Sandford S.A., 1998, J. Phys. Chem. 102, 353
Joblin C., Léger A., Martin P., 1992, ApJ 393, L79
Langhoff S.R., 1996, J. Phys. Chem. 100, 2819
Léger A., Puget J.L., 1984, A&A 137, L5
Léger A., Puget J.L., 1989, ARA&A 27, 161
Lepp S., Dalgarno A., 1988, ApJ 335, L769
Molster F.J., Waters L.B.F.M., Trams N.R., et al., 1999, A&A 350, 163
Molster, F.J., van den Ancker M.E., Tielens A.G.G.M., et al., 1996, A&A 315, L373
Moutou C., Léger A., d'Hendecourt L., 1996, A&A 310, 297
Moutou C., Verstraete L., Sellgren K., et al., 1999, In: Cox P., Kessler M.F. (eds.) The universe as seen by ISO. ESA-SP 427, p. 727
Peeters E., Tielens A.G.G.M., Roelfsema P.R., et al., 1999, In: Cox P., Kessler M.F. (eds.) The universe as seen by ISO. ESA-SP 427, p. 579
Roche P.F., Aitken D.K., Smith C.H., 1989, MNRAS 236, 485
Roelfsema P.R., Cox P., Tielens A.G.G.M., et al., 1996, A&A 315, L289
Schutte W., Tielens A.G.G.M., Allamandola L., 1993, ApJ 415, 397
Sylvester R.J., Kemper F., Barlow M.J., et al., 1999, A&A in press
Tielens A.G.G.M., Hony S., Van Kerckhoven C., et al., 1999, In: Cox P., Kessler M.F. (eds.) The universe as seen by ISO. ESA-SP 427, p. 579
Van Kerckhoven C.,Tielens A.G.G.M, Waelkens C., 1999, In: Cox P., Kessler M.F. (eds.) The universe as seen by ISO. ESA-SP 427, p. 421
Voors R.H.M, 1999, Ph.D. Thesis, Universiteit Utrecht, The Netherlands
Zhang K., Guo B., Colarusso P., et al., 1996, Sci 274, 582